Helicity structure of the Pomeron-nucleon-nucleon vertex using a multiperipheral model*

C. A. Wingate
Department of Physics, University of Illinois at Urbana-Champaign, Urbana, Illinois 61801
(Received 9 December 1976)

Using a version of the multiperipheral model, the Pomeron-nucleon-nucleon helicity residue functions are obtained over a wide range of t values. Pions are assumed to be exchanged along the sides of the multiperipheral ladder and all but the lowest helicity-determining loop are replaced by a Pomeron exchange. The helicity-flip-to-nonflip ratios are found to be in good agreement with experiment while the overall normalization is less than experiment. An interesting sign structure is found in the individual flip amplitudes for the exchanged baryons. A review is also given of the current experimental status of the helicity structure of πN and NN elastic scattering.

I. INTRODUCTION

It has long been suspected that in certain diffractive processes such as elastic scattering and vector-meson photoproduction s-channel helicity is conserved. The most convenient reactions used to study this phenomenon are ρ photoproduction, pion-nucleon and nucleon-nucleon elastic scattering. In this paper we model the Pomeron-nucleon-nucleon (P-N-N) vertex and compare the results to data from both πN and NN scattering. A similar model for vector-meson photoproduction is described in Fishbane and Sullivan (Ref. 1). Throughout this work we adopt a t-channel language and assume that the amplitudes are described by the exchange of one or more Regge trajectories.

The main purpose of this paper is to give a description of the helicity structure of the P-N-N vertex utilizing a version of the multiperipheral model. In order to isolate the contribution of the Pomeron to the amplitude we work in the asymptotic energy region. We take the viewpoint that Regge cuts, while being ultimately necessary, are not needed for the level of accuracy being considered here.

The basic idea of our model is illustrated in Fig. 1. In the multiperipheral ladder diagram for the specific πN elastic scattering [Fig 1(a)] we assume that the intermediate baryon state propagates along the lowest rung of the ladder. The rest of the ladder is taken to be composed of meson exchanges. Thus all of the pertinent helicity information is contained in the lowest loop of the ladder. Because of this, we do not need to be concerned with the remainder of the ladder. Since a calculation of the full ladder would generate a Regge exchange, we replace all but the lowest loop of the ladder with a Pomeron exchange as in Fig 1(b). This leaves a single-loop integral which completely determines the helicity structure of this πN scattering process. The elastic scattering process $NN \to NN$ is described in a similar manner.

Utilizing this procedure, we calculate the P-N-N residue function for various t values [$0 \leq |t| \leq 1$ (GeV/c)^2]. In particular, we obtain the helicity-flip-to-nonflip ratio of the P-N-N vertex which we compare directly to experiment.

The relative phase between the flip and nonflip amplitudes in this model is completely determined and real. The experimentally determined relative phase, however, is only known at low energy and at these energies is dependent on the interplay between the various possible Regge exchanges. Thus we will not compare our phase results with experiment.

The first calculation of this type to be done was carried out by Islam.[2] He calculated the s-channel

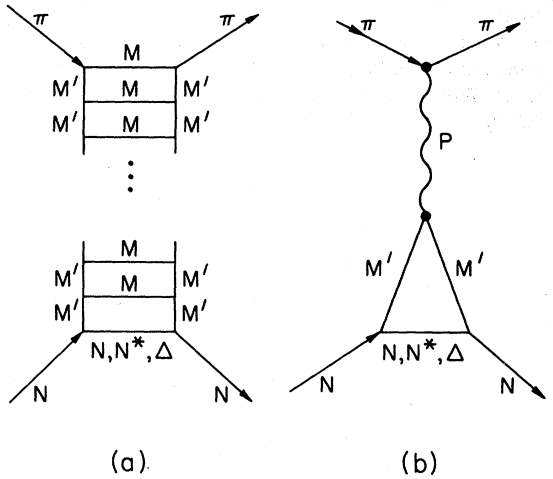

FIG. 1. (a) Multiperipheral ladder diagram for πN elastic scattering. M and M' are mesons. (b) Replacement of the upper part of the ladder with a Pomeron Regge trajectory (P).

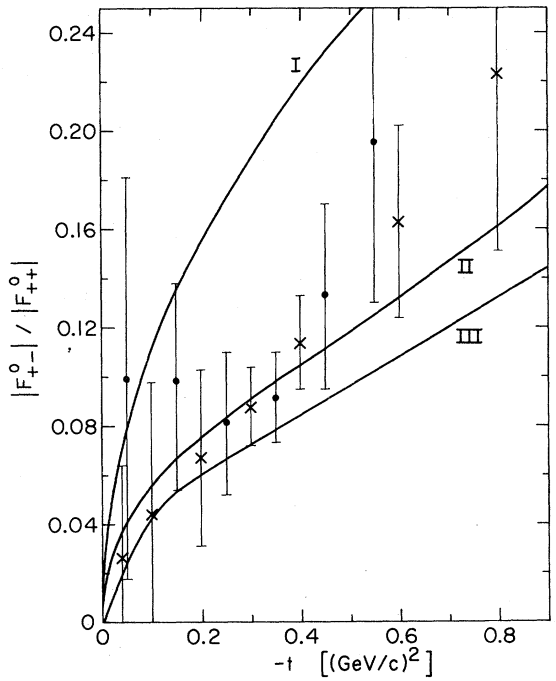

FIG. 2. Absolute value of the s-channel helicity-flip-to-nonflip ratio at $p_L = 6$ GeV/c versus the four-momentum transfer squared t for the isospin-0 exchanges in the t channel. The data points indicated by × are from Ref. 2 and those indicated by • are from Ref. 3. The parameters for the theoretical curves (discussed in Secs. III and IV) are curve I: $\Lambda^2 = 1$ (GeV/c)^2, $n = 1$ for spin $\frac{1}{2}$ and 2 for spin $\frac{3}{2}$; curve II: $\Lambda^2 = 1.4$ (GeV/c)^2, $n = 2$; curve III: $\Lambda^2 = 1.8$ (GeV/c)^2, $n = 2$.

helicity-nonflip amplitude F_{++} and the derivative of the flip amplitude $dF_{+-}/d\sqrt{-t}$ for πN elastic scattering at $t = 0$ only. Using a different method for calculating the lowest loop he demonstrated approximate s-channel helicity conservation for the very forward t region. A second calculation performed by Dash and Jones obtained Regge residue functions in πN and NN elastic scattering over a wide range of t.[3] They calculated the entire ladder assuming ρ exchanges along the rungs and only the $\Delta(1236)$ as the intermediate baryon state. As we see below, however, the contribution of the $N(939)$ intermediate state is equally important and is crucial for the helicity conservation which we obtain.

This paper is organized as follows: In Sec. II we review and summarize the experimental evidence for s-channel helicity structure in πN and NN elastic scattering. In particular, we determine the degree of helicity conservation at the P-N-N vertex. In Sec. III we present the details of the model we use for our theoretical calculations. A detailed description and motivation for this model in the context of vector-meson photoproduction is given in Fishbane and Sullivan (Ref. 1). Section IV is reserved for the results and conclusions.

II. EXPERIMENTAL EVIDENCE FOR HELICITY CONSERVATION AT THE P-N-N VERTEX

Pion-nucleon scattering is the most throughly studied of all scattering processes. Seven measurements at each energy and momentum transfer are necessary in order to determine the four complex spin and isospin amplitudes (up to an overall phase which must be determined in a different manner). The most convenient experimental quantities that one may use to determine the amplitudes are the three cross sections $(d\sigma/dt)^{+,-,0}$, the three polarizations $P^{+,-,0}$, and a spin rotation parameter R^- (or R^+). The superscripts +, −, and 0 refer to $\pi^+ p$ elastic, $\pi^- p$ elastic, and $\pi^- p \to \pi^0 n$ charge-exchange scattering, respectively.

In π-N scattering a complete set of experiments has been done at only one energy, $p_L = 6$ GeV/c. The R parameter measurement at this energy is described in Ref. 4. Following this latter experiment several model-independent analyses were carried out which determined the amplitudes up to an overall phase.[5-7]

Some of the results for the amplitudes corresponding to isospin-0 exchanges in the t channel are shown in Fig. 2. Both analyses shown in this figure used the same R measurement, but the analysis of Ref. 6 utilized more recent P^0 and $d\sigma/dt$ data. The quantity exhibited is the s-channel helicity-flip-to-nonflip ratio, $|F^0_{+-}|/|F^0_{++}|$, where the amplitudes $F^0_{\lambda\lambda'}$ are normalized according to $d\sigma/dt = |F_{++}|^2 + |F_{+-}|^2$. The superscript 0 on F denotes isospin 0 in the t channel. One sees that the $I_t = 0$ exchanges approximately conserve s-channel helicity, i.e., the flip-to-nonflip ratio at $t \approx -0.3$ (GeV/c)^2 is about 0.1 for $p_L = 6$ GeV/c (note that this ratio is constrained by angular momentum conservation to vanish at $t = 0$).

From the results at this one energy alone, it is impossible to separate the contribution of the Pomeron exchange from the other $I_t = 0$ exchanges. In spite of the fact that a complete set of measurements does not exist at any other energy, estimates based on incomplete data sets have been made at $p_L = 16$ and 40 GeV/c.[5,8] At 16 GeV/c several amplitude solutions are allowed by the available data. The ones which are most likely are those which correspond to $R^+ > R^-$ as is the case at 6 GeV/c. The composite range of these latter solutions is shown in Fig. 3. At 40 GeV/c if one assumes that (i) the charge-exchange nonflip amplitude may be neglected compared to the elastic nonflip amplitudes, and (ii) powers of $F_{+-}(\pi^- p)/F_{++}(\pi^- p)$ higher than the first are negligible, one may derive bounds

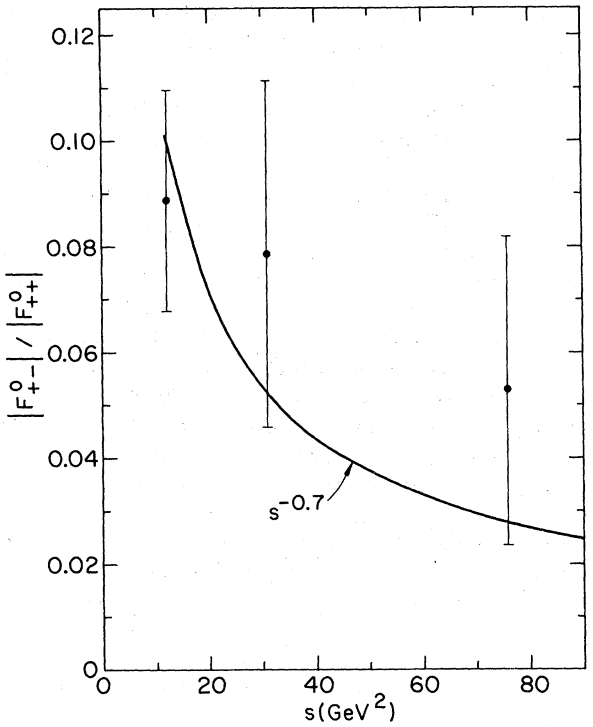

FIG. 3. Plot of s-channel helicity-flip-to-nonflip ratio, $|F^0_{+-}|/|F^0_{++}|$, versus center-of-mass energy squared s at $t=-0.33$ (GeV/c)^2. The data are from ($p_L=6$ GeV/c) Ref. 6, (16 GeV/c) Ref. 5, and (40 GeV/c) Ref. 8. The curve is $s^{\alpha_n}/s^{\alpha_P}$, $\alpha_P=1.0+0.3t$, and $\alpha_n=0.5+t$, normalized to 0.1 at $p_L=6$ GeV/c. This would be the approximate s dependence of the flip-to-nonflip ratio if $\beta^P_{+-}=0$.

on the flip-to-nonflip ratio. Figure 3 shows this at $t=-0.33$ (GeV/c)^2 as a function of s. The downward trend of the data is indicative of the presence of other $I_t=0$ trajectories in addition to the Pomeron. If this trend is smoothly continued out to very large s, where the lower-lying trajectories will be insignificant, we see that the Pomeron-flip-to-nonflip ratio might range from 0 to about 0.06 at this particular t value. Thus, while we cannot make a precise estimate of the Pomeron helicity-flip-to-nonflip ratio, we can place an upper bound on this ratio of about 10% which is compatible with all known πN scattering data.

The helicity structure of the P-N-N vertex may also be studied in p-p elastic scattering. In this process there are five complex amplitudes, thus requiring the measurement of nine independent quantities. At the present time the only measured quantities in the GeV energy range are the unpolarized cross section $d\sigma/dt$, the polarization P, the spin rotation parameter R, the depolarization parameter D_{nn}, the spin-spin correlation parameters C_{nn} and C_{ss}, and various spin-state cross-section measurements. Here n refers to a unit vector perpendicular to the scattering plane while s refers to a unit vector in the scattering plane perpendicular to the beam. The R, D_{nn}, C_{nn}, and C_{ss} data are described in Refs. 9, 10 and 11, respectively. The total and differential cross-section spin-state measurements at several s and t values and a measurement of the polarization transfer parameter K_{nn} at a single s and t value are described in Ref. 12. The relationship of these parameters to the five independent s-channel helicity amplitudes is given in Ref. 13. The experimental information thus far known is not enough to carry out a model-independent amplitude analysis. However, with the assumption of the Regge-pole model and factorization we can get an idea of how well s-channel helicity is conserved at the P-p-p vertex.

A very useful parameter for this purpose is the spin rotation parameter R which has been measured at $p_L=3.83$, 6, 16, and 45 GeV/c.[9] The experimental data for R at $p_L=45$ GeV/c are shown in Fig. 4. These data contain contributions from the Pomeron, other $I_t=0$ Regge exchanges, and $I_t=1$ Regge exchanges. To determine how well the data are fitted by a Pomeron exchange and to test the sensitivity of the resulting curves

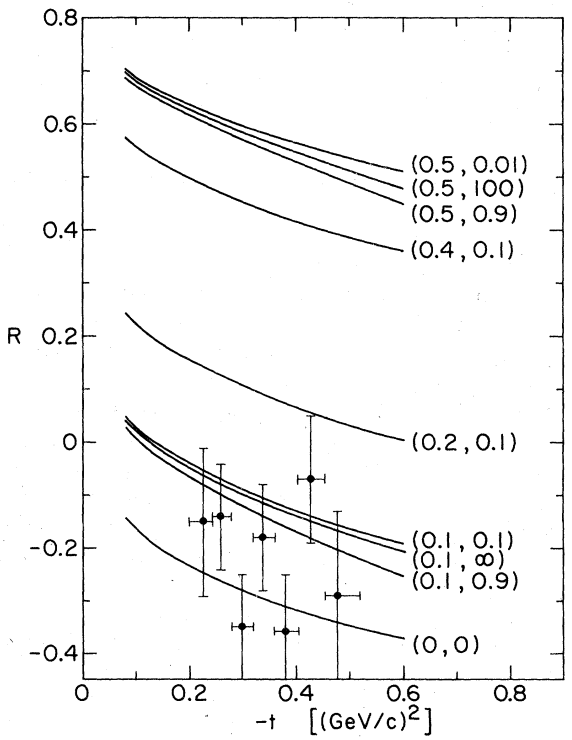

FIG. 4. The spin rotation parameter R for pp elastic scattering at $p_L=45$ GeV/c as a function of t. The parameter associated with the theoretical curves are (X^P, X^ρ), where $X^i=\beta^i_{+-}/\beta^i_{++}$.

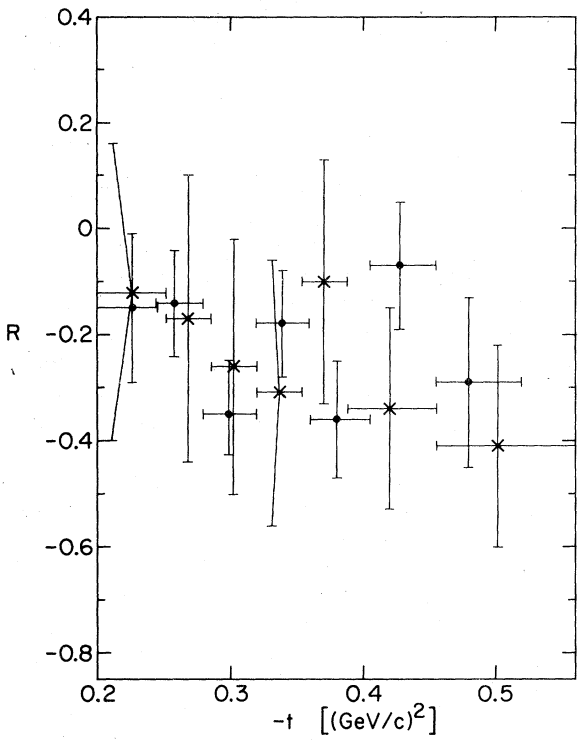

FIG. 5. The R parameter for pp elastic scattering versus t for $p_L = 3.83$ (×) and 45 (●) GeV/c. The data are taken from Ref. 9.

to the inclusion of $I_t = 1$ exchanges, we assume that two Regge exchanges contribute to the amplitude at this energy—the Pomeron and a composite $I_t = 1$ exchange denoted by ρ. With the further assumption of factorization it is possible to draw a family of curves in Fig. 4 which depend only on the two parameters $X^i = \beta^i_{+-}/\beta^i_{++}$, $i = P$, or ρ where $\beta^i_{\lambda_1\lambda_2}(t)$ is the corresponding Regge vertex function. The ratio X^i should contain the kinematical factor $\sqrt{-t}$, but for simplicity X^i is chosen to be constant. The parameter $\beta^P_{++}(t)$ is determined from the pp elastic differential cross section[14] at $s \sim 3000$ GeV^2 while $\beta^\rho_{++}(t)$ is determined from the $pn \to np$ charge-exchange differential cross section.[15] The two parameters associated with each curve in Fig. 4 are (X^P, X^ρ).

We can also attempt to determine the sensitivity of the R parameter to $I_t = 0$ Regge exchanges other than the Pomeron by studying the energy dependence of R. The data for R at $p_L = 3.83$ and 45 GeV/c are shown in Fig. 5. It is clear that the currently available data do not permit a meaningful separation of the Pomeron and other $I_t = 0$ low-lying trajectories.

The C_{nn} parameter also provides information about the helicity structure of the P-N-N vertex. Medium-energy data for C_{nn} exist at $p_L = 2$, 3, 4, 6, and 12 GeV/c.[11] The data at 6 and 12 GeV/c are shown in Fig. 6. If we assume a single Pomeron exchange and factorization then

$$C_{nn} = \frac{4X^P(t)^2}{1 + X^P(t)^2} . \tag{1}$$

By taking $X^P(t)$ from the data for πN scattering we generate the curve drawn in Fig. 6.

The conclusions we can draw from the data and curves shown in Figs. 4 and 6 are:

(i) There are not yet sufficient p-p data to extract the t dependence of the helicity-flip-to-nonflip ratio of the Pomeron.

(ii) The curves in Fig. 4 indicate that the R data at $p_L = 45$ GeV/c are consistent with the $I_t = 0$ exchanges collectively conserving s-channel helicity to 20% or better. We also see that a reasonable admixture of the $I_t = 1$ exchange does not significantly alter this conclusion.

(iii) The R parameter experiments, although done over a relatively wide range, are not accurate enough to separate the P from lower-lying trajectories.

(iv) The C_{nn} data, while not reproduced well by a Pomeron exchange alone, and consistent with a helicity-flip-to-nonflip ratio $X^{I=0}(t) \lesssim 0.20$.

Thus we see that one gets a consistent picture of

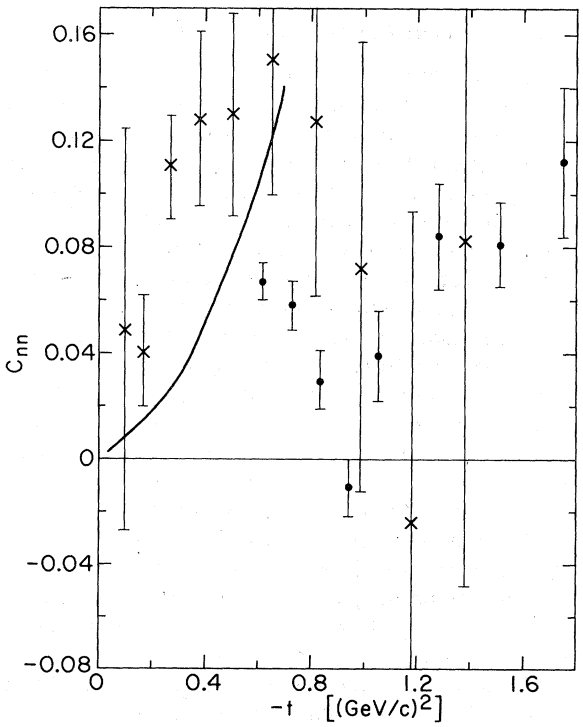

FIG. 6. C_{nn} versus t at $p_L = 6$ (×) and 12 (●) GeV/c. The curve is calculated by assuming a single Regge exchange, i.e., the Pomeron. The data are from Ref. 11.

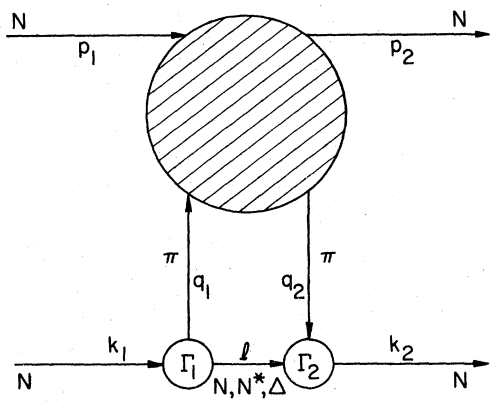

FIG. 7. Feynman diagram for N-N elastic scattering in the multiperipheral model. The blob represents all the upper rungs of the ladder.

the P-N-N vertex from both the pp and πp data, and that the latter process provides the sharpest results on the P-N-N vertex. For the helicity-flip-to-nonflip ratio we take the data exhibited in Fig. 2 with the realization that this includes significant contributions from other exchanges. Remembering the s dependence shown in the data of Fig. 3, we suspect that the true Pomeron-flip-to-nonflip ratio will be somewhat lower than the data in Fig. 2.

III. MULTIPERIPHERAL MODEL FOR THE P-N-N VERTEX

In this section we calculate the s-channel helicity amplitudes in the asymptotic energy region within the framework of a multiperipheral model using π exchanges on the sides of the multiperipheral ladder. In particular, we calculate the P-N-N vertex functions over a range of t values $[0 \leq |t| \leq 1$ (GeV/$c)^2]$. For definiteness our calculations are carried out for nucleon-nucleon scattering. However, since factorization is implicit in our model, P-N-N vertex functions at any t will be the same for the elastic scattering of any particle on a nucleon. For the same reason we may average over the helicity values along one of the nucleon lines when carrying out our calculations for N-N elastic scattering.

From our results for the spin dependence on one of the nucleon lines it is easy to calculate the full spin dependence of the N-N amplitudes. For example, the helicity amplitude $H_1 = \langle{+}{+}\,|\,{+}{+}\rangle$ is simply proportional to the square of our nonflip residue function.

The basic diagram for this calculation is shown in Fig. 7. A convenient choice of kinematical variables for this process is enumerated in Ref. 1. Only the lowest loop of the ladder is shown because this is the part which determines the helicity structure of the lower vertex. The rest of the ladder, which builds up the diffractive behavior of the amplitude, is treated as an input, as described above, by replacing it with a Pomeron Regge exchange.

We calculate the diagram with pion exchange along the sides, because it is assumed that this constitutes a large portion of the amplitude. Since we are using as input on-the-mass-shell pion-nucleon scattering in place of virtual pion-nucleon scattering it is necessary to include pion form factors in the expressions for the amplitudes. The parameters describing these form factors are essentially the only arbitrary items in the calculation and will be discussed in more detail below.

The intermediate baryon state in Fig. 7 (momentum l) is taken to be either a $J^P = \frac{1}{2}^+$ or a $\frac{3}{2}^+$ state. Both $I = \frac{1}{2}$ and $\frac{3}{2}$ states are included. Exclusion of the known higher-spin intermediate states ($J \geq \frac{5}{2}$) and any unknown but presumably higher-mass states is not completely justifiable *a priori*. For the nonflip amplitude, however, examination of the results (see Table I) shows that all contributions are of the same sign and that the lower-mass intermediate states, in particular the $N(939)$ and $\Delta(1232)$, are dominant. The flip amplitude, on the other hand, could, in certain instances, depend very critically on contributions from higher-mass intermediate states. This occurs because the helicity-flip amplitudes enter with a mixture of signs (see Table I). In particular, for suitable choices

TABLE I. The P-N-N vertex functions at $t = -0.1$ (GeV/$c)^2$ for the various intermediate baryon resonances. The input parameters are $\alpha_P = 1.0 + 0.3t$, $\Lambda^2 = 1$ (GeV/$c)^2$, $n = 1$ for spin-$\frac{1}{2}$ states and 2 for spin-$\frac{3}{2}$ states.

Intermediate state	J^P	Nat.	γ_{++}	γ_{+-}	γ_{+-}/γ_{++}
$N(939)$	$\frac{1}{2}^+$	+	128.5	32.15	0.25
$N(1470)$	$\frac{1}{2}^+$	+	20.8	4.55	0.22
$N(1780)$	$\frac{1}{2}^+$	+	1.6	0.30	0.19
$\Delta(1910)$	$\frac{1}{2}^+$	+	1.3	0.24	0.18
$N(1535)$	$\frac{1}{2}^-$	−	1.2	−0.13	−0.11
$\Delta(1650)$	$\frac{1}{2}^-$	−	0.7	−0.07	−0.10
$N(1700)$	$\frac{1}{2}^-$	−	2.4	−0.24	−0.10
$\Delta(1232)$	$\frac{3}{2}^+$	−	51.5	−21.15	−0.41
$N(1810)$	$\frac{3}{2}^+$	−	1.4	−0.44	−0.31
$N(1520)$	$\frac{3}{2}^-$	+	15.0	9.11	0.61
$\Delta(1670)$	$\frac{3}{2}^-$	+	2.2	1.19	0.54
Totals			226.6	25.51	0.11

of the pion form factors, it is possible to achieve almost complete cancellation in the flip amplitude between the dominant low-mass states $N(939)$, $N(1470)$, $\Delta(1232)$, and $N(1520)$. In this case the higher-mass intermediate states will make the controlling contribution to the flip amplitude. As a practical matter, however, with the cancellation of the lower-mass states the resultant flip amplitude will have a very small value.

By utilizing the recursive structure of the multiperipheral model, the amplitude corresponding to Fig. 7 can be written as

$$M^{J^P}_{\lambda_1\lambda_2} = \int \frac{d^4l}{(2\pi)^4} \tilde{M} L^{J^P}_{\lambda_1\lambda_2} F(q_1^2) F(q_1^2), \tag{2}$$

where λ_1 and λ_2 are the initial and final nucleon helicities, respectively. The index J^P refers to the spin parity of the intermediate baryon state. The factor L includes the spinor factors associated with the lower baryon line as well as the exchanged pion propagators. It is written down using standard Feynman rules:

$$L^{J^P}_{\lambda_1\lambda_2} = \Phi(4\mu_1\mu_2)^{1/2}\left(\frac{i}{q_1^2 - M_1^2}\right)\left(\frac{i}{q_2^2 - M_2^2}\right) \times \bar{u}_{\lambda_2}(-ig_2\Gamma_2^J) S_J (-ig_1\Gamma_1^J) u_{\lambda_1}, \tag{3}$$

where

$$\Gamma_i^{1/2} = 1 \text{ for } \tau_i\tau_0 = -\Big\}, \quad i = 1, 2,$$
$$\Gamma_i^{1/2} = \gamma_5 \text{ for } \tau_i\tau_0 = +\Big\}$$

τ = naturality = parity $\times (-1)^{J-1/2}$,

Φ = isospin factor,

$$S_{1/2} = \frac{i(\not{l} + \mu_0)}{l^2 - \mu_0^2},$$

$$(S_{3/2})_{\mu\nu} = \frac{i(\not{l} + \mu_0)}{l^2 - \mu_0^2}\left(-g_{\mu\nu} + \tfrac{1}{3}\gamma_\mu\gamma_\nu + \frac{2}{3}\frac{l_\mu l_\nu}{\mu_0^2} + \frac{l_\nu\gamma_\mu - l_\mu\gamma_\nu}{3\mu_0}\right),$$

$$\Gamma_i^{3/2} = \begin{cases} k_{1\mu}\Gamma_1^{1/2}, & i = 1 \\ k_{2\nu}\Gamma_2^{1/2}, & i = 2, \end{cases}$$

and $\bar{u}u$ is normalized to 1.

In Eq. (2) $\tilde{M}$ is the input πN elastic scattering amplitude. It is represented by the Regge exchange of a Pomeron

$$\tilde{M} = -\beta(t) s'^{\alpha_P}\left(\frac{1 + e^{-i\pi\alpha_P}}{\sin(\pi\alpha_P)}\right), \tag{4}$$
$$\beta(t) = \beta_0 e^{b\pi t/2},$$
$$s' = (p_1 + q_1)^2.$$

This particular form for $\beta(t)$ is chosen because, for diffractive scattering, the differential cross section is a rapidly falling exponential of t (for small t) with a well-defined slope parameter b. The coefficient β_0 is obtained from the total cross section for πN elastic scattering.

We choose for the form factor $F(q_i^2)$ in Eq. (2) the two-parameter form

$$F(q_i^2) = \left(1.0 - \frac{q_i^2 - M_i^2}{\Lambda^2}\right)^{-n}, \tag{5}$$

where M_i is the mass of the particle exchanged along the side of the ladder. We assume that the major contribution to the amplitude comes from pions near the mass shell. Using this as a guide the parameters we choose are $\Lambda^2 \approx 1.0$ (GeV/c)^2 and $n = 1$ or 2. For convergence of the integral in the spin-$\frac{3}{2}$ case $n = 2$ is required.

In our actual work we calculate the s-channel discontinuity of the amplitude, $\text{Disc}_s(M) = [M(s + i\epsilon, t) - M(s - i\epsilon, t)]$, rather than the amplitude itself. This effectively reduces the number of integrals in Eq. (2) from four to three. For more details on this procedure, see Ref. 1. The resulting three integrals are calculated numerically using Gaussian quadrature. The full amplitude M is then reconstructed from $\text{Disc}_s(M)$ by the simple formula

$$M = -\left(\frac{1 + e^{-i\pi\alpha_P}}{\sin(\pi\alpha_P)}\right)\frac{\text{Disc}_s(M)}{2i}. \tag{6}$$

IV. RESULTS

Table I gives a breakdown of the contributions by intermediate baryon resonance to the P-N-N vertices $\gamma_{\lambda_1\lambda_2}$ at $t = -0.1$ (GeV/c)^2. The vertex functions are related to the absorptive parts of the amplitude by

$$\lambda_{\lambda_1\lambda_2} = 8.2 e^{1.8t}\text{Disc}_s(M_{\lambda_1\lambda_2})/(2is^{\alpha_P}), \tag{7}$$

where the numerical factors come from the spin average of the upper vertex. One interesting feature of the results shown in Table I is the fact that the sign of the flip absorptive amplitude is always equal to the naturality of the intermediate baryon resonance. This result holds for all values of Λ^2, n, and t thus far investigated [$0.001 \le \Lambda^2 \le 10^2$ (GeV/c)^2, $1 \le n \le 4$, $0 \le t \le -3.0$ (GeV/c)^2]. Moreover, one notes that the flip-to-nonflip ratios for the individual intermediate states varies from about 0.1 to 0.6 with the major contributions being about 0.25 from the $N(939)$ and 0.41 from the $\Delta(1232)$. When all the states are added together, however, cancellation among the contributions to the flip amplitude brings the final ratio down to about 0.11, in general agreement with experiment.

The t dependence of the flip-to-nonflip ratio, γ_{+-}/γ_{++}, is shown by the curves in Fig. 2 along with the experimental data. One sees from this that with the appropriate and reasonable choices of the form-factor parameters Λ^2 and n we can approximately reproduce the t dependence of the data.

In contrast to the good agreement between the

ratios, the model prediction for the N-N total cross section differs from the experimental value. Using the same input parameters that were used in calculating Table I, we determine that the total N-N cross section is 28.1 mb. This is about $\frac{3}{4}$ of the experimental N-N total cross section at high energy ($\sigma_{pp} \approx 40$ mb). We note that by increasing the form-factor parameter Λ^2 we can increase the model prediction for the total cross section. In fact, for $\Lambda^2 \gtrsim 1.5$ (GeV/c)^2, $n=1$ for spin-$\frac{1}{2}$ states and $n=2$ for spin-$\frac{3}{2}$ states, the model total cross section is already greater than the experimental total cross section.

In order to satisfy both requirements that the flip-to-nonflip ratio be consistent with experiment and that the π-exchange total cross section be less than the experimental total cross section we need to choose form-factor parameters of $\Lambda^2 = 1.8$ (GeV/c)^2, $n=2$ for both spin-$\frac{1}{2}$ and spin-$\frac{3}{2}$ intermediate states. The t dependence of the flip-to-nonflip ratio for these choices is shown in Fig. 2. The total cross section corresponding to these parameters is about 36 mb.

In a multiperipheral ladder calculation of this type one might ask about double counting. This occurs when, in the course of doing the loop integral in Fig. 7, the bottom baryon rung plus one or more of the meson rungs contained within the Pomeron can have an invariant mass equal to a higher-mass baryon resonance. Thus in the spirit of duality it might be argued that there is no need to include higher-mass baryon resonances as the bottom rung of Fig. 7. However, the meson rungs and the bottom baryon line are connected only once by un-Reggeized pion exchange. This seems insufficient to generate the full resonance. In fact, the interplay between the twin principles of unitarity and duality has not yet been fully resolved. The multiperipheral approach used here is based primarily on the unitarity relation. It is not surprising, therefore, that implications of duality are not clear at present. For these reasons we have chosen to explicitly include all the baryon resonances in our calculations ignoring the possible (hopefully small) double-counting effects.

We conclude from the results of the above calculation that the π-exchange multiperipheral process contributes a large fraction of the total N-N amplitude. This is to be contrasted with the calculations of ρ photoproduction in Ref. 1, where the π-exchange multiperipheral contribution represented only about 0.3 of the experimental amplitude. The remainder of the N-N amplitude presumably comes from the exchanges of higher-mass particles along the sides of the multiperipheral ladder.

We also see that, since the π flip-to-nonflip ratio is approximately equal to the experimental ratio, the aggregate flip-to-nonflip ratio for the other exchanges must conserve s-channel helicity to the same degree. Furthermore, we conjecture that each individual exchange approximately conserves s-channel helicity. It would also be interesting to determine if the other amplitudes exhibit the same sign pattern in the intermediate baryon contributions to the flip amplitude as in the π exchange.

ACKNOWLEDGMENT

The author wishes to thank Dr. J. D. Sullivan for many helpful discussions.

*Work supported in part by NSF under Grant No. PHYS 75-21590.

[1] P. M. Fishbane and J. D. Sullivan, unpublished work.
[2] S. Islam, Nucl. Phys. B41, 226 (1972).
[3] J. W. Dash and S. T. Jones, Phys. Rev. D 11, 1817 (1975).
[4] A. de Lesquen *et al.*, Phys. Lett. 40B, 277 (1972).
[5] G. Cozzika *et al.*, Phys. Lett. 40B, 281 (1972).
[6] I. Ambats *et al.*, Phys. Rev. D 9, 1179 (1974).
[7] F. Halzen and C. Michael, Phys. Lett. 36B, 367 (1971); P. Johnson *et al.*, Phys. Rev. Lett. 30, 242 (1973); R. L. Kelly, Phys. Lett. 39B, 635 (1972); M. Giffon, Nuovo Cimento 7A, 705 (1972).
[8] J. Pierrard *et al.*, Phys. Lett. 57B, 393 (1975).
[9] J. Deregel *et al.*, Nucl. Phys. B103, 269 (1976); J. Deregel *et al.*, Phys. Lett. 43B, 338 (1973); J. Pierrard *et al* , *ibid.* 61B, 107 (1976).
[10] G. W. Abshire *et al.*, Phys. Rev. D 12, 3393 (1975).
[11] G. Hicks *et al.*, Phys. Rev. D 12, 2594 (1975); D. Miller *et al.*, Phys. Rev. Lett. 36, 763 (1976); K. Abe *et al.*, Phys. Lett. 63B, 239 (1976); I. P. Auer *et al.*, Phys. Rev. Lett. 37, 1727 (1976); 38, 258 (E) (1977).
[12] E. F. Parker *et al.*, Phys. Rev. Lett. 31, 783 (1973); W. de Boer *et al.*, *ibid.* 34, 558 (1975); J. R. O'Fallon *et al.*, *ibid.* 32, 77 (1974); R. C. Fernow *et al.*, Phys. Lett. 52B, 243 (1974); this group also measured D_{nn} at one s and t value.
[13] E. Leader and R. C. Slansky, Phys. Rev. 148, 1491 (1966).
[14] G. Barbiellini *et al.*, Phys. Lett. 39B, 663 (1972).
[15] H. R. Barton *et al.*, in *Particles and Fields—1975*, proceedings of the meeting of the Division of Particles and Fields of the American Physical Society, Seattle, edited by H. J. Lubatti and P. M. Mockett (Univ. of Washington, Seattle, 1976), p. 424.